

faces of humans and sheepdogs than to sheep or other animal faces (see Fig. 4C). There was also a slight tendency for these cells to respond to horned animals. Lastly, two cells responded similarly to a number of different faces including those of animals such as pigs. All cells responding to faces responded much less, or not at all, to upside-down faces. On a few occasions facial profiles of sheep were shown and these also evoked similar, although generally smaller, responses compared with the faces shown frontally. The response latencies of these cells responding to faces were short: between 80 and 180 msec (median 120 msec) and the responses did not generally outlast the period of stimulus presentation. A total of 56 other visually responsive cells were found in the temporal cortex that responded to movement, usually in a specific direction, of any object either in the contralateral visual field (46 cells) or in both ipsi- and contralateral fields (10 cells). A further 25 cells responded to auditory cues and 10 cells responded to somatosensory cues (touching of areas of the head and face). None of these cells, or those responding to faces, were polysensory, however.

These results demonstrate that facial recognition cells in the temporal cortex are not unique to primates. As in the monkey (1), these cells have short response latencies suggesting that they are primarily involved in sensory processing rather than in motor responses to these stimuli. However, unlike the monkey (1), they do not respond to upside-down faces, which seems reasonable since, unlike monkeys, sheep do not usually view other sheep upside down. Different groups of facial recognition cells code for different features known from behavioral studies to be socially significant. One group of cells codes selectively for the presence and size of horns, possibly allowing for a rapid estimation of the perceived animal's sex or position in the dominance hierarchy. A second group of cells may code for animals of the same breed and for familiarity. A third group of cells appears to code for potential threatening stimuli, such as humans and dogs. These results provide an important insight into the way the brain can rapidly code complex visual information in terms of appropriate behavioral responses.

REFERENCES AND NOTES

1. C. Bruce, R. Desimone, C. G. Gross, *J. Neurophysiol.* **46**, 369 (1981); C. G. Gross, C. E. Rocha-Miranda, D. B. Bender, *ibid.* **35**, 96 (1972); D. I. Perrett, E. T. Rolls, W. Caan, *Exp. Brain Res.* **47**, 329 (1982).
2. G. C. Baylis, E. T. Rolls, C. M. Leonard, *Brain Res.* **342**, 91 (1985); R. Desimone, T. D. Albright, C. G. Gross, C. Bruce, *J. Neurosci.* **4**, 2051 (1984); D. I. Perrett *et al.*, *Proc. R. Soc. London Ser. B* **223**, 293 (1985).
3. D. I. Perrett *et al.*, *Aspects of Face Processing*, H. Ellis

- and M. A. Jeeves, Eds. (Nijhoff, Dordrecht, 1986), p. 187; E. T. Rolls, *Brain Mechanisms of Sensation*, Y. Katsuki, R. Norgren, S. Sato, Eds. (Wiley, New York, 1981), p. 241; D. I. Perrett *et al.*, *Human Neurobiol.* **3**, 197 (1984).
4. H. Kluver and P. C. Bucy, *Arch. Neurol. Psychiatry* **42**, 979 (1939).
 5. C. G. Gross, *Handbook of Sensory Physiology*, R. Jung, Ed. (Springer, Berlin, 1973), vol. 7/3B, p. 451; P. Dean, *Psychol. Bull.* **83**, 41 (1976).
 6. J. C. Meadows, *J. Neurol. Neurosurg. Psychiatry* **37**, 489 (1974); A. M. Whiteley and E. K. Warrington, *ibid.* **40**, 394 (1977).
 7. P. G. H. Clarke and D. Whitteridge, *J. Physiol. (London)* **256**, 497 (1976); P. G. H. Clarke, I. M. L. Donaldson, D. Whitteridge, *ibid.*, p. 509.

8. E. Shillito Walser, S. Willadsen, P. Hague, *Appl. Anim. Ethol.* **7**, 351 (1981); C. G. Winfield and P. D. Mullaney, *Anim. Prod.* **17**, 93 (1973).
9. G. Alexander and E. E. Shillito, *Appl. Anim. Ethol.* **3**, 137 (1977).
10. V. Geist, *Z. Tierpsychol.* **25**, 199 (1968); *Mountain Sheep: A Study in Behaviour and Evolution* (Univ. of Chicago Press, Chicago, 1971).
11. N. E. Collias, *Ecology* **37**, 228 (1956); G. A. Lincoln, *J. Exp. Zool.* **182**, 233 (1972).
12. K. M. Kendrick and B. A. Baldwin, *Brain Res.* **375**, 320 (1986).
13. J. E. Skinner, *Neuroscience: A Laboratory Manual* (Saunders, Philadelphia, 1971).

3 December 1986; accepted 13 March 1987

A Small Gold-Conjugated Antibody Label: Improved Resolution for Electron Microscopy

JAMES F. HAINFELD

A general method has been developed to make the smallest gold-conjugated antibody label yet developed for electron microscopy. It should have wide application in domainal mapping of single molecules or in pinpointing specific molecules, sites, or sequences in supramolecular complexes. It permits electron microscopic visualization of single antigen-binding antibody fragments (Fab') by covalently linking an 11-atom gold cluster to a specific residue on each Fab' such that the antigenic specificity and capacity are preserved. The distance of the gold cluster from the antigen is a maximum of 5.0 nanometers when the undecagold-Fab' probe is used as an immunolabel.

THE USE OF ANTIBODIES TO MARK molecules or tissues specifically has been an important tool in structural biology. Visualization of these antibody labels in the electron microscope (EM) has usually required conjugation either with an electron-dense moiety such as ferritin (1) or colloidal gold (2). Although these procedures are adequate for some studies, these labels are generally too large for submolecular mapping, which is unfortunate since monoclonal antibodies to various determinants on a molecule are available. The antibody molecule (3) is ~15 nm in diameter, and the Protein A-colloidal gold complex is ~12 to 35 nm in diameter or larger, so that a conjugated label (4) has a diameter of ~27

to 50 nm. An antibody label 1/5 to 1/10 the size of those currently available has now been synthesized. It is formed by coupling an antigen-binding antibody fragment (Fab') to an undecagold (Au₁₁) complex such that antigenic binding capacity is retained. The Fab' fragment is 50 kD and is 5.0 by 4.0 by 3.0 nm in size (5). The undecagold complex has a core that is 0.8 nm in diameter and is composed of 11 gold atoms (with an organic shell that is ~0.6 nm thick). The core is easily visible in the scanning transmission electron microscope (STEM). The maximum dimension of the

Biology Department, Brookhaven National Laboratory, Upton, NY 11973.

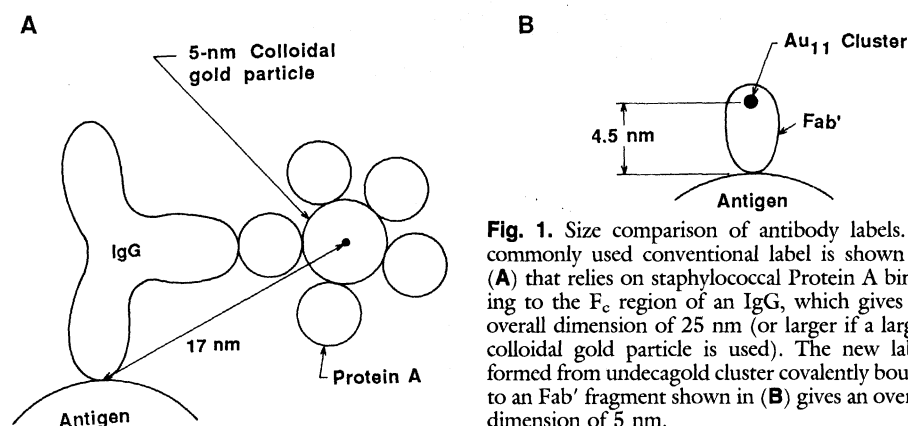


Fig. 1. Size comparison of antibody labels. A commonly used conventional label is shown in (A) that relies on staphylococcal Protein A binding to the Fc region of an IgG, which gives an overall dimension of 25 nm (or larger if a larger colloidal gold particle is used). The new label formed from undecagold cluster covalently bound to an Fab' fragment shown in (B) gives an overall dimension of 5 nm.

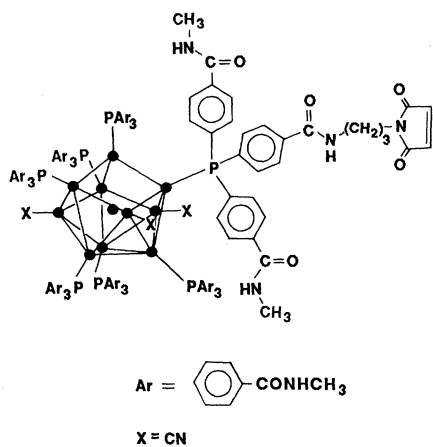


Fig. 2. Monofunctional undecagold cluster. It has a dense core (0.8 nm in diameter) of 11 gold atoms that is surrounded by an organic shell. The single maleimide group specifically reacts with free sulfhydryls. The coordinating counterion is represented as X.

conjugated undecagold-Fab' as measured from micrographs is ~ 5.4 nm. This means that the Au_{11} marker could be at most 5.4 nm from the antigenic site, but the actual distance in this study was ≤ 5.0 nm (Fig. 1).

This much smaller antibody label should be useful for discerning specific sites on single protein molecules or nucleic acid chains. Also, the small size of this label should permit labeling of some secluded sites that are inaccessible to larger labels. Although Fab fragments alone have previously been used as EM labels (6), this has been done only with ordered arrays with image processing, since the individual Fab molecules in general cannot be directly discerned. Unconjugated immunoglobulin G (IgG) molecules have also been used to label single ribosomes (7), but this technique requires a favorable viewing angle such that the antibody is on the periphery; otherwise its position is obscured. The undecagold-Fab' label would be advantageous since the gold core is visible even on top of a 20-nm-wide molecule.

The undecagold complex (8) is water soluble and can be covalently linked through its external organic shell to specific residues or molecules. It was used to determine the position of biotin sites on avidin molecules to ~ 1.0 -nm resolution. This level of resolution had not been achieved previously in labeling isolated molecules (9). Another reaction was used to specifically mark carbohydrate moieties on a glycoprotein (10). More recently, Safer *et al.* (11) and Reardon and Frey (12) have independently synthesized new forms of the undecagold complex that are monofunctional. This monofunctionality is important because polymerization often occurred in labeling attempts with the original multifunctional undeca-

gold. One of these new monofunctional undecagold complexes was used in these experiments. Its structure is shown in Fig. 2. The one maleimide group that will react directly with free sulfhydryls is indicated.

Fab' fragments (50 kD) can be prepared that have one free sulfhydryl group at a location distant from the antibody-antigen binding region (13). Martin *et al.* demonstrated that only one free sulfhydryl group was produced (with rabbit IgG) and used this to attach Fab' fragments to lipid vesicles. Antibody fragments coupled in this way were found to retain full antigenic specificity and capacity. This method was adapted for gold cluster labeling as outlined in Fig. 3.

The labeled Fab' molecules are shown in Fig. 4, A and B. The labeling was quantitative; each Fab' fragment bound usually one undecagold cluster, but sometimes two or three (and rarely four). Unusually reactive amines can cause labeling of additional sites. Less likely possibilities were that other disulfides could have been reduced, or some gold clusters could have formed oligomers. Gold clusters on 724 Fab' molecules were counted to determine a more exact stoichiometry. The mean was found to be 1.5 ± 0.7 (SD) clusters per Fab'. A spectral assay of the Fab'- Au_{11} complex in solution indicated a stoichiometric ratio of 1.4 Au_{11} to 1 Fab'. The undecagold cluster on the Fab' was

located in the same place on each Fab' molecule (at one end), as expected from the position of the free sulfhydryl group. When two undecagold clusters were found on an Fab' fragment, the second site was always 1.8 to 2.8 nm from the first, which again indicated specific attachment. Similarly, when a third undecagold cluster was present, it was 1.8 to 2.8 nm from the first; the three clusters usually formed a triangular cap (sometimes they formed a linear array) on one end of the Fab' molecule. The undecagold clusters were always localized at one end of the Fab' molecule. Some of these multiply labeled Fab' fragments could be identified when they were bound to the antigen and therefore did not appear to affect antibody activity.

Mass analysis of labeled Fab' particles that were randomly selected was done with a computer from micrographs with the elastically scattered electron signal (14, 15). The values in kilodaltons from 96 particles had a mean of 56.5 ± 13.9 SD. The expected weight was 57.5 kD (50 kD for Fab' + 7.5 kD for the average of 1.5 undecagolds per Fab'); each undecagold has a molecular weight of 5 kD; this agreement confirms identification of the antibody fragment.

The IgG used was rabbit antibody to horse ferritin. To demonstrate that the gold-labeled Fab' fragments retained their antibody activity, they were mixed in 20-fold

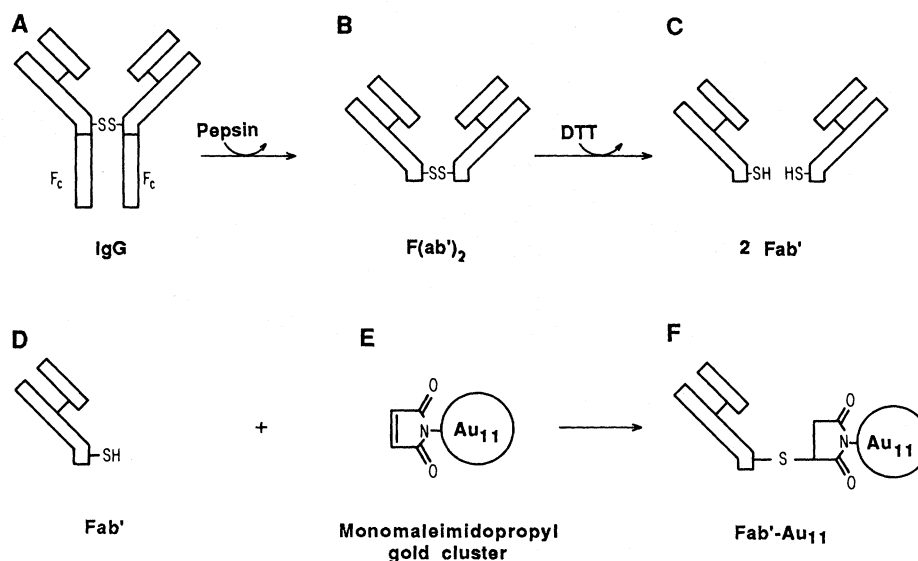
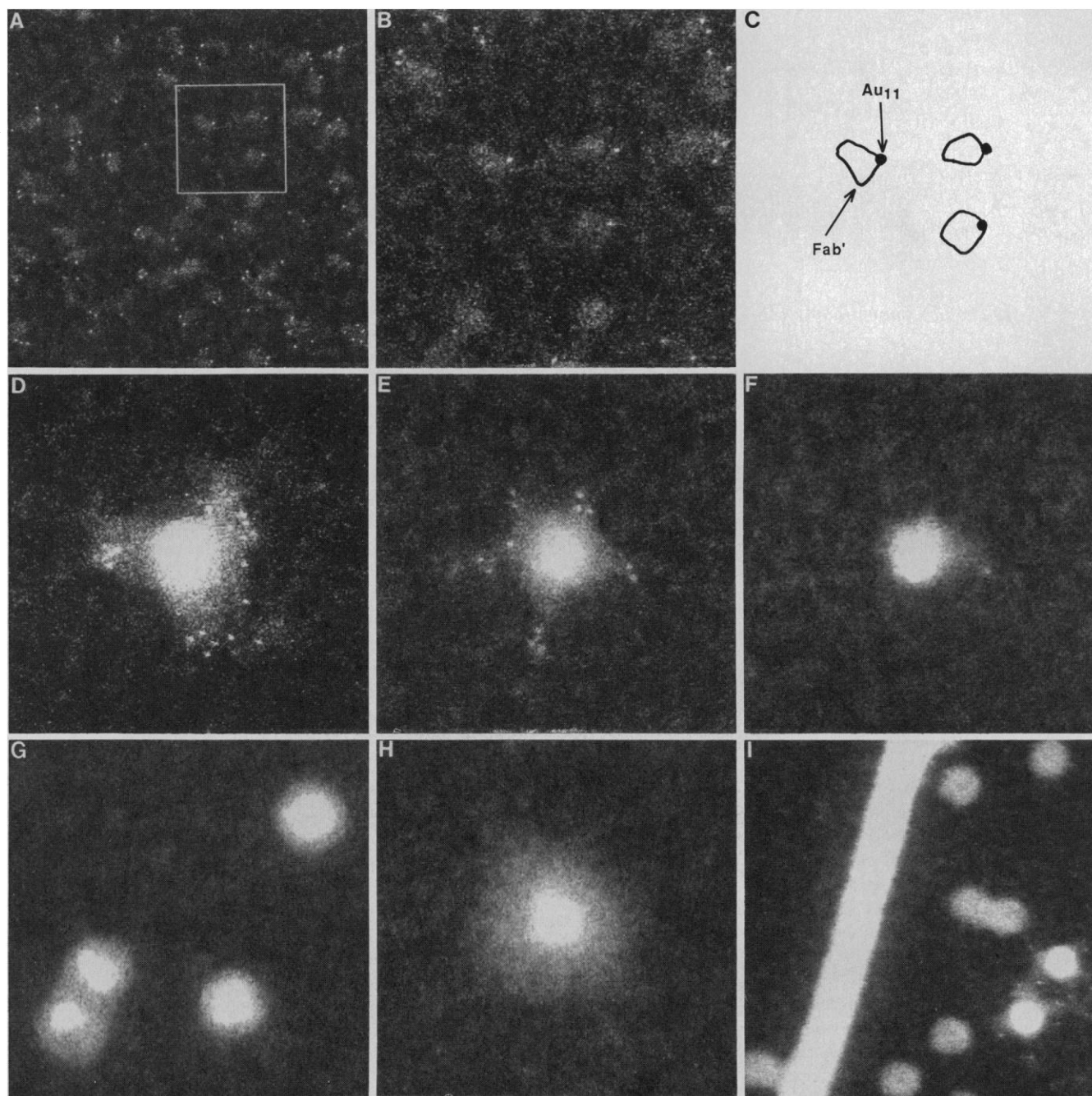


Fig. 3. Reaction scheme for labeling Fab' with undecagold. Rabbit IgG (from Cooper Biomedical, Inc.) was digested with pepsin to yield $F(ab')_2$ fragments joined by a disulfide (A and B). The constant fragment (F_c) regions were removed by a Staph A-Sepharose column; other digested fragments were removed on a high-pressure liquid chromatography (HPLC) Fractogel TSK HW-55 (S) column. Next 20 mM dithiothreitol (DTT) was used to reduce the disulfide link (B and C), which produced the Fab' fragment (2-hour reaction time under N_2). DTT was removed with the HPLC column. After each pass through the column, protein was concentrated to 0.5 to 1.0 mg/ml with Amicon Centricon 10 microconcentrators. Undecagold was activated immediately before use by reaction of monoaminopropyl- Au_{11} and *N*-methoxycarboxyl maleimide to form monomaleimidopropyl- Au_{11} (E). The product was purified on a carboxylic CM Sepharose column (11). The Fab' and activated Au_{11} were incubated overnight at 4°C (D to F). Unreacted Au_{11} was removed with an HPLC Fractogel TSK HW-40(S) column. Protein was applied to EM grids and freeze-dried overnight before observation in the STEM (14).



molar excess with horse ferritin; each ferritin molecule has a shell of 24 similar subunits that encapsulate the 8.0-nm-diameter core of iron oxides (16). After a 1-hour incubation, any unbound material was eliminated by passage through a TSK-HW55(S) high-pressure liquid chromatography column.

Several examples of ferritin molecules with bound Fab'-Au₁₁ molecules are shown in Fig. 4, D through F. In these images, the halo around the bright iron core is the shell of the ferritin protein which has a diameter of 12.5 nm. Protrusions with similar density (the Fab' proteins) can be seen; the 0.8-nm undecagold clusters appear as the bright spots at the periphery. The maximum distance of the gold clusters from the edge of

the ferritin molecules is 5.0 nm; some clusters are much closer. These clusters at closer proximity may be bound to subunits out of the plane, thus causing them to appear closer to the ferritin core than they actually are. The number of Au₁₁ clusters that could be counted per ferritin molecule was 7.3 ± 3.8 SD (207 molecules examined) and varied from 0 to 21. If a gold cluster was above or below the iron core, it would not have been easily distinguished, so this number probably underestimates the amount of label that was bound. The ferritin shell has 432 symmetry (16) and frequently views of Fab'-Au₁₁-labeled ferritin show some indication of symmetry, such as the roughly threefold view in Fig. 4D. Although poly-

clonal antibodies were used in this study, the use of monoclonal antibodies might be used to elucidate the underlying symmetry of a structure. Note that ferritin is normally used as an EM label, but with this technique it is labeled with a marker whose electron-dense core is 1/10 the size of the ferritin core.

The rabbit IgG used in this study has only one disulfide in the hinge region of the antibody (13) that was used for labeling with the undecagold cluster. Human antibodies have between 2 and 15 disulfides in the hinge region, most of which remain after pepsin digestion (17). Conceivably, the use of human Fab' fragments could dramatically increase the loading of undecagold, which would make the fragments easily visible in

Fig. 4 (left). Undecagold-labeled Fab' fragments are shown in (A). The Fab' molecules show quantitative labeling and the undecagold spots (0.8 nm in diameter) are at one end of these 50-kD fragments. Some Fab' fragments show more than one Au₁₁ cluster attached. Three clear fragments, each with one gold cluster attached, can be seen in the boxed region. This vicinity is enlarged two times in (B); a simple schematic is shown in (C). Typical ferritin molecules with gold-labeled Fab' fragments attached are shown in (D) and (E). The binding of a single Fab'-Au₁₁ complex to a ferritin molecule is shown in (F) for clarity. Controls are shown in (G to I): Rabbit antibody to dynein Fab'-Au₁₁ molecules (not shown) was prepared and appeared to be similar to (A) and was reactive toward dynein. When this Fab'-Au₁₁ was incubated with ferritin and passed through a column, only native ferritin was found (G). Activated and unactivated gold clusters (with a maleimide or an amine group at the end of the linking arm) were separately incubated with ferritin, then separated on a column. Images similar to (G) were obtained, which indicated that no gold bound to the ferritin. Spectral absorbance of the gold was also used to determine that no gold had bound. Antibody to ferritin Fab' (with no gold attached, but with the free sulfhydryl blocked with *N*-ethyl maleimide) was incubated in excess with ferritin. A subsequent incubation with antibody to ferritin Fab'-Au₁₁ (and column separation) showed no gold cluster spots on the ferritin since all epitopes had been exhausted. The unlabeled Fab' around the ferritin is clearly seen in (H) as an additional shell of protein density. When antibody to ferritin Fab'-Au₁₁ was incubated with tobacco mosaic virus (TMV), glutamine synthetase (GS), and ferritin, only the ferritin was labeled (I). TMV is the rod-shaped object; GS molecules are the round, medium-intensity objects about the same diameter as TMV. Two ferritin molecules are at the lower right with dense cores and have several Fab'-Au₁₁ labels attached. All incubations were for 1 hour at 37°C. Images were recorded with the STEM in the dark-field mode at a dose of 0.60 e nm⁻². Full width: 106 nm (A and I); 53 nm (B to H).

thin sections or in conventional EMs without a sacrifice of the high resolution of this technique.

Other antibodies have been successfully labeled by this technique and include: rabbit antibody to flagella, rabbit antibodies to 22S dynein and 14S dynein, and two mouse monoclonal antibodies to bovine factor V. This indicates that the labeling procedure described should be generally applicable to many antibodies.

REFERENCES AND NOTES

1. S. J. Singer, *Nature (London)* **183**, 1523 (1959).
2. W. P. Faulk and G. M. Taylor, *Immunochimistry* **8**, 1081 (1971).
3. R. Huber, J. Deisenhofer, P. M. Colman, M. Matsu-shima, W. Palm, *Nature (London)* **264**, 415 (1976).
4. E. L. Romano and M. Romano, *Immunochimistry* **14**, 711 (1977).
5. R. J. Poljak, L. M. Amzel, H. P. Avey, L. N. Becka, A. Nisonoff, *Nature (London) New Biol.* **235**, 137 (1972).
6. U. Aebi et al., *Proc. Natl. Acad. Sci. U.S.A.* **74**, 5514 (1977).
7. M. R. Wabl, *J. Mol. Biol.* **84**, 241 (1974).
8. J. S. Wall et al., *Ultramicroscopy* **8**, 397 (1982).

9. D. Safer, J. F. Hainfeld, J. S. Wall, J. E. Reardon, *Science* **218**, 290 (1982).
10. J. J. Lipka, J. F. Hainfeld, J. S. Wall, *J. Ultrastruct. Res.* **84**, 120 (1983).
11. D. Safer, L. Bolinger, J. S. Leigh, *J. Inorg. Biochem.* **26**, 77 (1986).
12. J. E. Reardon and P. A. Frey, *Biochemistry* **23**, 3849 (1984).
13. F. J. Martin, W. L. Hubbell, D. Papahadjopoulos, *ibid.* **20**, 4229 (1981).
14. M. W. Mosesson, J. Hainfeld, R. H. Haschemeyer, J. S. Wall, *J. Mol. Biol.* **153**, 695 (1981).
15. J. S. Wall and J. F. Hainfeld, *Annu. Rev. Biophys. Biophys. Chem.* **15**, 355 (1986).
16. G. C. Ford et al., *Philos. Trans. R. Soc. London Ser. B* **304**, 551 (1984).

17. P. D. Gorevic, *Methods Enzymol.* **116**, 3 (1985).
18. I thank D. Safer for synthesizing and providing the undecagold reagent; K. D. Elmore, I. M. Feng, Y. L. Wang, and G. G. Shieu for technical assistance; S. Marchese-Ragona for the gift of antibody to dynein IgG; S. Trachtenberg for providing antibody to flagella; W. Church for antibody to factor V; J. S. Wall, J. J. Lipka, H. W. Siegelman, and P. S. Furciniti for helpful discussions; and F. E. Kito and M. N. Simon for operation of the STEM. This work was supported by the Office of Health and Environmental Research of the Department of Energy and by NIH grant GM 31975.

22 September 1986; accepted 4 February 1987

Efficacy of Murine Malaria Sporozoite Vaccines: Implications for Human Vaccine Development

JAMES E. EGAN,* JAMES L. WEBER, W. RIPLEY BALLOU, MICHAEL R. HOLLINGDALE, WILLIAM R. MAJARIAN, DANIEL M. GORDON, W. LEE MALOY, STEPHEN L. HOFFMAN, ROBERT A. WIRTZ, IMOGENE SCHNEIDER, GILLIAN R. WOOLLETT, JAMES F. YOUNG, WAYNE T. HOCKMEYER†

As part of a study of potential vaccines against malaria, the protective efficacy of sporozoite subunit vaccines was determined by using the *Plasmodium berghei* murine malaria model. Mice were immunized with recombinant DNA-produced or synthetic peptide-carrier subunit vaccines derived from the repetitive epitopes of the *Plasmodium berghei* circumsporozoite gene, or with radiation-attenuated sporozoites. Immunization with subunit vaccines elicited humoral responses that were equivalent to or greater than those elicited by irradiated sporozoites, yet the protection against sporozoite challenge induced by either of the subunit vaccines was far less than that achieved by immunization with attenuated sporozoites. Passive and adoptive transfer studies demonstrated that subunit vaccines elicited predominantly antibody-mediated protection that was easily overcome whereas irradiated sporozoites induced potent cell-mediated immunity that protected against high challenge doses of sporozoites. These studies indicate that new strategies designed to induce cellular immunity will be required for efficacious sporozoite vaccines.

IMMUNIZATION WITH SPOROZOITES attenuated by irradiation protects animals and humans from experimental sporozoite-induced malaria (1). This finding, first with *Plasmodium berghei* in rodents and subsequently with the human malaria species *P. falciparum* and *P. vivax*, provided great impetus to the development of human sporozoite vaccines. The characterization of sporozoite membrane antigens that play a role in the development of this immunity revealed a family of circumsporozoite (CS) proteins that have a general structure common to all malaria species studied to date (2). The gene for the CS protein of *P. falciparum*, for example, contains a long stretch of nucleotide base pairs that are highly conserved among different strains of the parasite (3) and encode a large central immunodominant repeat region with the amino acid sequence Asn-Ala-Asn-Pro (4). Antibodies elicited by immunization with synthetic peptides derived from this repeat region neutralize sporozoite infectivity, but antibodies elicited by immunization with

synthetic peptides derived from two nonrepeat regions that are highly conserved among malaria species do not (5). The CS protein repeat sequences have thus been identified as the major target for malaria vaccine development.

There is considerable evidence that antibody to the CS protein has a role in sporozoite-induced immunity. Passive transfer of

J. E. Egan, J. L. Weber, W. R. Ballou, D. M. Gordon, W. T. Hockmeyer, Department of Immunology, Walter Reed Army Institute of Research, Washington, DC 20307.

M. R. Hollingdale and G. R. Woollett, Biomedical Research Institute, Rockville, MD 20852.

W. R. Majarian and J. F. Young, Department of Molecular Genetics, Smith Kline French Laboratories, Swedeland, PA 19479.

W. L. Maloy, Biological Resources Branch, National Institute of Allergy and Infectious Diseases, National Institutes of Health, Bethesda, MD 20872.

S. L. Hoffman, Malaria Branch, Naval Medical Research Institute, Bethesda, MD 20814, and Department of Immunology, Walter Reed Army Institute of Research, Washington, DC 20307.

R. A. Wirtz and I. Schneider, Department of Entomology, Walter Reed Army Institute of Research, Washington, DC 20307.

*To whom correspondence should be addressed.

†Present address: Praxis Biologics, 300 East River Road, Rochester, NY 14623.